$\pi^{\pm}$ Charge Exchange Cross Section on Liquid Argon*

Kevin Nelson *REU Program, College of William and Mary*

Mike Kordosky *College of William and Mary, Physics Dept.*

August 5, 2016

Abstract

The observation of neutrino oscillations[1] allows charge parity violation to be probed in the neutrino sector. Detectors with high calorimetric energy resolution and high spatial resolution will provide precise measurements of neutrino oscillations. By measuring small $\pi^{\pm}$ cross sections for individual interaction channels, specifically charge exchange, we will make a measurement in the first of its kind on liquid Argon and demonstrate the physics capabilities of a relatively new detector technology: the Liquid Argon Time Projection Chamber (LAr TPC). This analysis will report on the cross section measurement technique of dividing the TPC into thin slabs to create an area for $\pi^{\pm}$ flux measurements. We will also report on Monte Carlo cross section measurements in the energy range of 0.2 - 1.0 GeV. This analysis is the first iteration in classifying charge exchange events from a sample of incident pions, and it aims to identify events in which a π^0 was produced without any charged pions leaving the interaction vertex. The algorithm works by finding the decay products of a π^0, photons, and tracing them back to the upstream interaction vertex of an incident $\pi^{\pm}$, as well as classifying tracks leaving the incident vertex as either $\pi^{\pm}$ or protons, and rejecting $\pi^{\pm}$. The algorithm was tuned on Monte Carlo simulations and can report a purity of 61% and an efficiency of 8.5% in the accepted sample of charge exchange events. This analysis will inform a future measurement of the $\pi^{\pm}$ charge exchange cross section on liquid argon.

*This work was supported in part by the National Science Foundation under Grant No. PHY-1359364.

1 Introduction

1.1 The LArIAT TPC

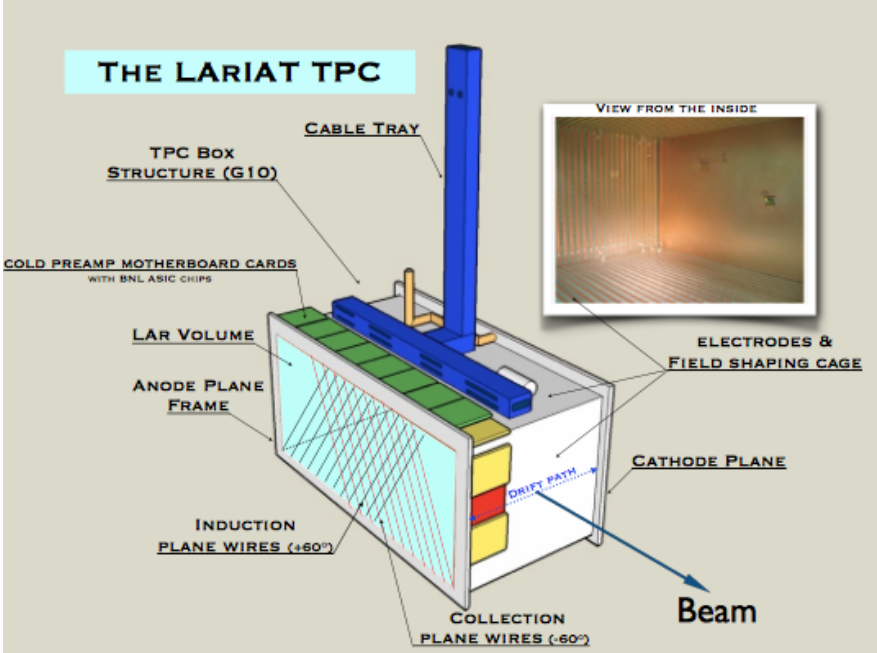

Figure 1: The LArIAT TPC [2]

The Liquid Argon in a Testbeam (LArIAT) Time Projection Chamber (TPC) (figure 1) is housed at the Fermi National Accelerator Laboratory (Fermilab) test beam facility. The chamber has two instrumented wire planes: the induction and collection plane. Both planes see drift electrons ionized from Argon atoms by charged particles moving within the TPC. Electrically neutral particles are not detectable in this TPC. Precise trigger timing is achieved by with the LArIAT beamline setup show in figure 2b, and allows for the measurement of drift time for ionization electrons, which move opposite the electric field between the anode and cathode planes. With a known trigger time, a known drift time, and a known constant drift velocity, a drift distance can be projected from the anode plane. Thus, the LArIAT detector has fully three-dimensional reconstruction capabilities for the motion of any charged particle in the TPC. The ability of our detector to accurately reconstruct the motion of charged particles is assumed for this analysis. The position resolution for particles in the beam direction is 4.62 mm, and varies with the angle of the motion relative to the angle of

the induction and collection wires.

The testbeam is composed of a range of charged species seen in figure 2a. Dipole magnets focus and bend the beam towards the TPC, as seen in figure 2b. The Run II data consists of varying magnet currents (to vary incident particle momentum) and two magnet polarities, positive and negative, to focus positive and negative species on the detector. Time of flight is calculated using an upstream and downstream detector, while series of wire chambers (MWPCs) calculate the bend in the beam from the magnets, yeilding a particle momentum. A combination of time of flight and momentum information gives a particle identification for incident beam particles. Knowledge of the species of the incident particle is critical to cross section measurements, and this has already been established in the LArIAT codebase. Therefore I will not address it any further and this analysis will assume that the incident particle has been correctly identified.

1.2 Cross Sections

A cross section is the effective area of a particle, used as an analog for the likeliness of a particle to interact. Neutrinos have tiny cross sections, and can move through significant amounts of matter without interacting. Protons and other hadronic particles have much larger cross sections, and generally travel on the order of centimeters before interacting in many forms of matter, including liquid Argon. Theoretically, the only quantities needed to calculate a cross section are particle flux and target's (in this analysis, nucleons) number density per unit area (nz). The probability of survival for a particle passing through matter in the z direction is an exponential decay function (the more matter a particle moves through, the less likely it is to survive):

$$P_{Survival} = e^{-\sigma nz} \tag{1}$$

The probability of interacting is the probability that the particle does not survive:

$$P_{Interacting} = 1 - P_{Survival} \tag{2}$$

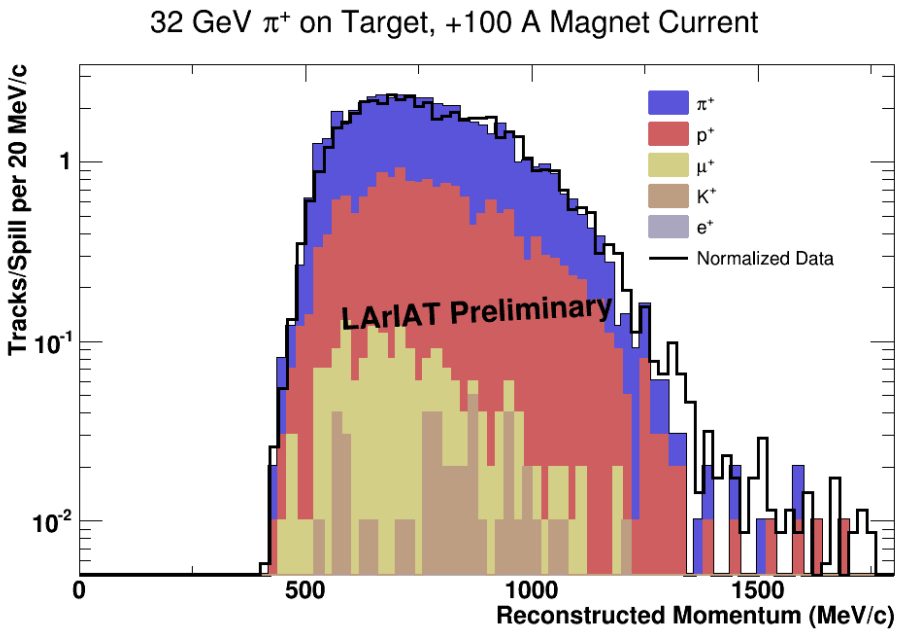

(a) Monte Carlo simulations on beam composition and data on beam intensity

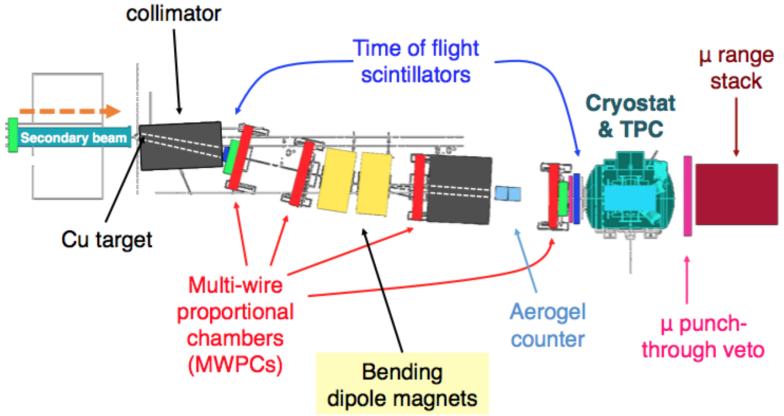

(b) The many detector devices of the LArIAT beamline

Figure 2: The LArIAT beam

and the empirical interaction probability is expressed as a counting measurement.

$$\frac{N_{Interacting}}{N_{Incident}} = P_{Interacting} = 1 - e^{\sigma nz} \tag{3}$$

Finally, a Taylor expansion is applied to the exponential,

$$P_{Interacting} = 1 - (1 - \sigma nz + ...) \tag{4}$$

and the equation is solved for the energy dependent cross section measurement.

$$\sigma(E) \approx \frac{1}{nz} \frac{N_{Interacting}}{N_{Incident}} \tag{5}$$

The particle flux is represented by a counting operation of the number of interacting and incident particles, which will allow an experimental measurement technique to be outlined in section 3.1.2.

2 Motivation

2.1 Operationally Defining Charge Exchange

The working definition of cross section for this analysis is a primary interaction (the furthest interaction upstream in the detector, for energy reconstruction concerns), in which a $\pi^{\pm}$ is incident and a π^0 is produced, while no $\pi^{\pm}$ exit the interaction vertex. As discussed in section 1.1, the ability for our detector to discern particle species and incident momentum from the beamline has been established. Therefore, finding π^0 production vertexes is half of the remaining analysis required to identify charge exchange events, aside from ensuring no $\pi^{\pm}$ exit the vertex.

As seen in figure 3[1], the π^0 product of a charge ex-

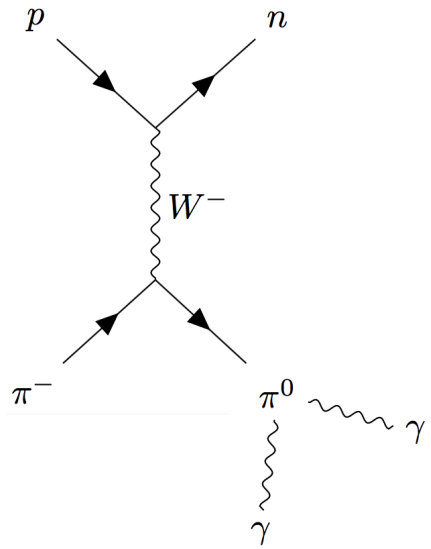

Figure 3: Feynman diagram of a π^--proton charge exchange interaction

[1]Feynman diagram generated using Tikz-Feynman[3]

change interaction decays nearly instantaneously into two photons. Photons are not directly detectable, but produce characteristic electromagnetic showers when they pair-produce or interact with the orbitals of the liquid argon atoms. The expected output from a charge exchange vertex is an number of nucleons and two photons. No charged pions are allowed to exit the vertex in this working definition of charge exchange, the "consumption" of the initial pion is required. See example event images in figures 4 (for signal) and 5 (for background).

3 Procedure

3.1 Measuring Monte Carlo Cross Sections

The first half of the procedure focused on measuring a Monte Carlo total cross section and charge exchange cross section for $\pi^{\pm}$-Argon.

3.1.1 Monte Carlo Simulations

This analysis made use of a monte carlo simulation of the LArIAT detector with a sample of 10,000 π^{-}. The knowledge of particle species and input momentum is not a bad approximation for real data, as discussed in section 1.1. However, the simulation also provided important information regarding the particle's interaction type and location, as well as the kinetic energy along the particle's motion, which all must be matched in reconstruction in order to produce data-driven measurements.

3.1.2 Thin Slab Technique

Before discussing the counting operation of the thin slab technique, I will derive the number density per unit area of nucleons in liquid Argon. The number density is calculated via the atomic weight (A) of Argon, Avogadro's number (N_A), and the density of liquid Argon[2] (ρ).

[2]Liquid Argon Properties retrieved from Particle Data Group[4]

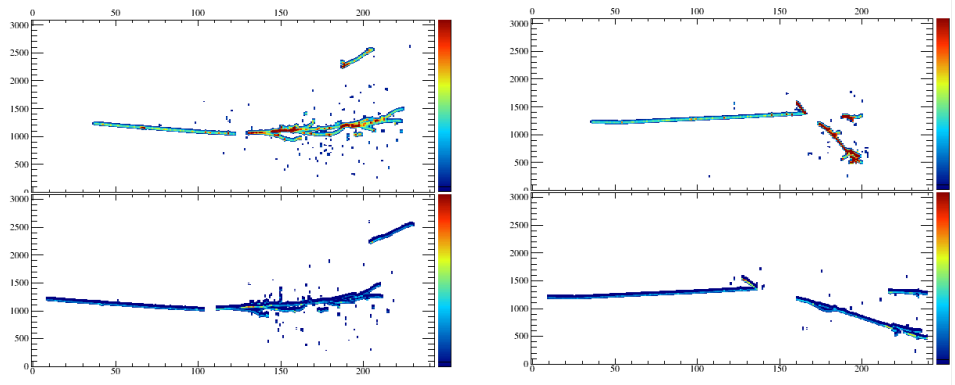

(a) Example signal event 1 (b) Example signal event 2

Figure 4: Two example signal events. The presence of two photons is a good indication of a π^0, but both are not always detected. Any particles leaving the interaction vertex are not $\pi^{\pm}$, and are likely protons from the Argon nucleus

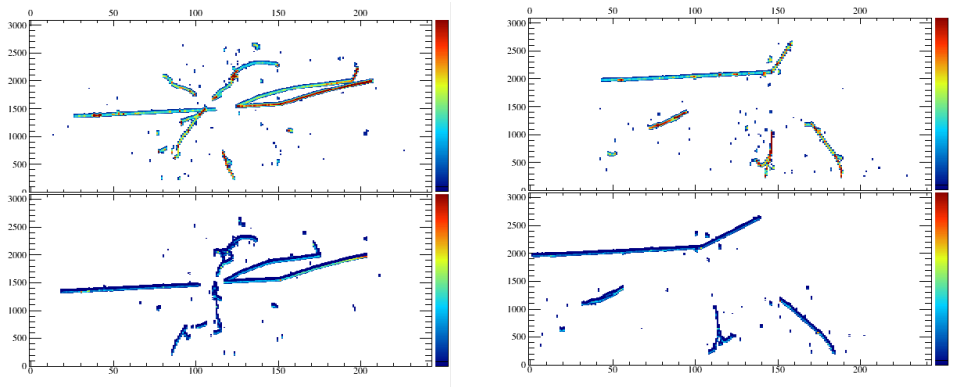

(a) Example background event 1 (b) Example background event 2

Figure 5: Two example background events. The first event is a kaon production event, which can mimic π^0 to our algorithm because there are electromagnetic decay products. The second has a charged pion exiting the interaction vertex, which would need to be discriminated against a proton

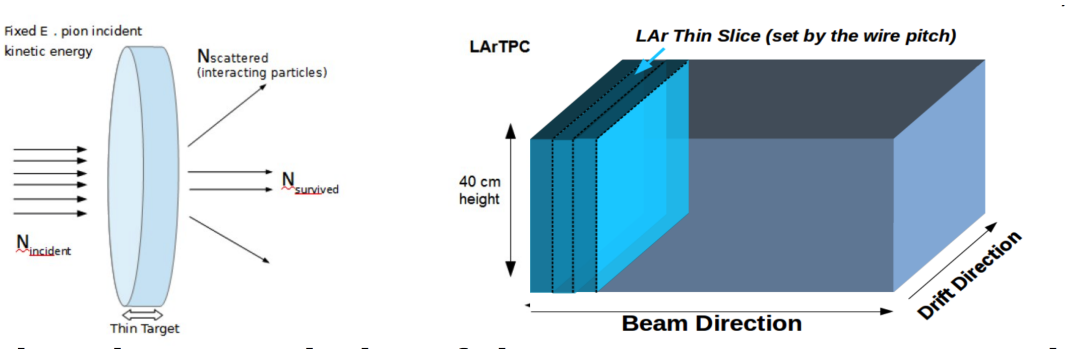

Figure 6: Diagram of flux counting scheme using the thin slab method

$$
\begin{aligned}
n &= \frac{\rho N_A}{A} \\
&= \frac{1.4\ grams}{cm^3}\frac{mol}{40\ grams}\frac{6.022\times 10^{23}\ nucleons}{mol}\frac{cm^2}{10^{24}\ barns} \\
&= 0.0211\frac{nucleon}{barn\times cm}
\end{aligned}
\tag{6}
$$

The thin slab technique divides the time projection chamber into a series of 1 cm-thick slabs, and uses the face of each as an area, over which a flux can be measured. The thickness of the slab was informed by the wire spacing. With a defined slab thickness, the constant $\frac{1}{nz}$ can be calculated:

$$
\frac{1}{nz} = 47.44\frac{barns}{nucleon} \tag{7}
$$

All that is left for cross section measurements is flux counting using the thin slab method. At each slab plane in the beam direction (see figure 6), a track is sampled to be either "incident", meaning it has not yet interacted, or "interacting" at the slab plane nearest its endpoint. At each slab plane the energy is interpolated from Monte Carlo. By counting the number of incident and interacting particles at various energies, and pairing this data with the constant nz derived above, the cross section is calculated by equation 5.

The technique for cross section measurement is no different for monte carlo or real data, except where queried information is retrieved from, simulation or data. Therefore, by producing a reliable algorithm for measuring simulated cross sections, we have also produced a reliable method for

measuring data cross sections, as will be done in a future analysis.

3.2 Identifying π^0 Production

3.2.1 Tracking Algorithms

Tracking algorithms are a part of LArIAT's codebase. The basic spatial reconstruction includes hit finding and signal smoothing on individual wires, clustering of hits in individual wire planes, merging clusters from different wire views into three dimensional points (the time projection element), and tracking through three dimensional points. Additionally, LArIAT has adopted a shower-finding algorithm from DUNE that identifies photon and electron-induced electromagnetic showers. In short, track and shower objects are produced that map trajectory and direction of particles. Shower objects are useful for finding photons and electrons, and track objects are useful for finding $\pi^{\pm}$, K, and protons.

3.2.2 Vertex Finding

Vertex finding is the first major endeavor of this analysis in identifying π^0 production. The upstream interaction vertex is the location of the first interaction of the incident $\pi^{\pm}$, and is useful because it is separated from the beamline momentum calculation described in section 1.1 by no intermediate interactions. Therefore it is the interaction that we know the most about: the species and momentum is known from the beamline (although some momentum will be lost, but this can be calculated using energy deposition information stored in a track object). A vertex can sometimes be (and often is) identified by the termination of a track. However, upon inspecting the simulation scattering at small angles is often overlooked by the track finding algorithm. We created a methodology of iterating along a track's set of points and measuring the angle of any interior track point with respect to its two neighbors. If the angle exceeds some cut value, then it is a kink in the track and the first such kink is the primary interaction vertex. The angle cut value was optimized to produce the best agreement between simulated interaction vertexes and reconstructed interaction vertexes. For results on the agreement between the two, see section 4.2.

3.2.3 Photon Identification

With a vertex established, the decay products of a π^0 can be identified. To establish that a π^0 was produced at the vertex, the algorithm searches for a shower object who's direction is very close to the vector between the vertex and shower origin, which we will call the production hypothesis vector. Showers that have too large an angle between the production hypothesis and the shower object's direction are rejected. The specific cut value was optimized to reject as many unrelated shower objects (those not inheriting directly from the vertex in question, assessed via Monte Carlo), while accepting as many signal showers as possible. If any reconstructed shower objects pass the cut, then the event is accepted as having π^0 production.

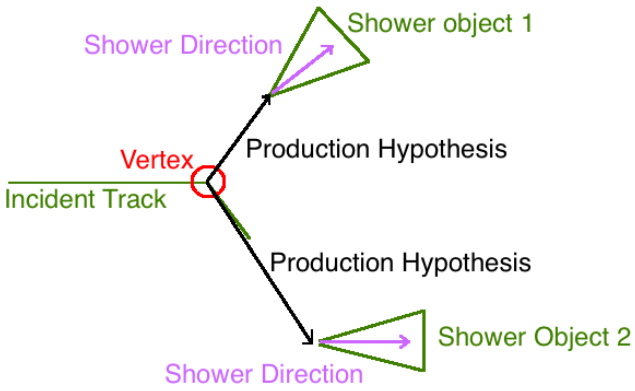

Figure 7: Shower finding procedure compares the angle of shower direction to the angle of the production hypothesis. Shower object 1 would potentially meet the cut requirements because it has a small angle between the production hypothesis vector and the shower's reconstructed direction. Shower object 2 would not meet the cut

It is important to note that π^0 particles decay into two photons. However, in the current iteration only one photon is required to accept an event. This is because the LArIAT detector is relatively small compared to the radiation length in liquid Argon. A particle produced in the center of the TPC has the nearest wall at 20 cm away, compared to a radiation length of 14 cm.

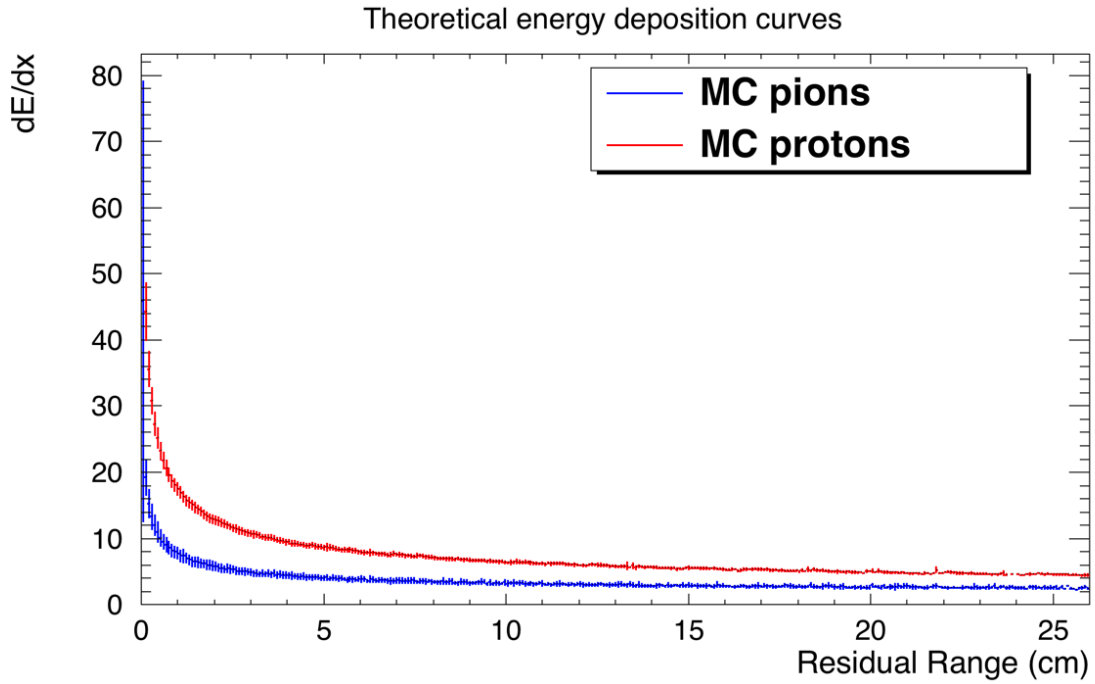

Figure 8: Theoretical energy deposition curves as a function of residual range, the distance to the track endpoint

Many photons will escape the TPC before pair-producing and creating a shower that the TPC can measure. Therefore, in order to accept as many π^0 events as possible, only a single photon meeting the defined cut is required.

3.3 $\pi^{\pm}$-proton Discrimination

In order to classify events as charge exchange or not, the criteria of no charged pions exiting the interaction vertex must be addressed. The LArIAT code-base has a built in particle identification algorithm that assigns a likelihood to pion and proton hypothesis based on energy deposition as a function of residual range. The theoretical distributions are shown in figure 8. Residual range is the distance from any track point to the track's endpoint, and is a good analog for momentum for stopping tracks. However, the LArIAT detector is small and many tracks are not stopping. Therefore, this method will have its limitations.

The algorithm functions by assigning a χ^2 value to a set of points from a track by comparing it to the pion and proton hypotheses. My classifier takes the difference in χ^2 as a cut value. Figure

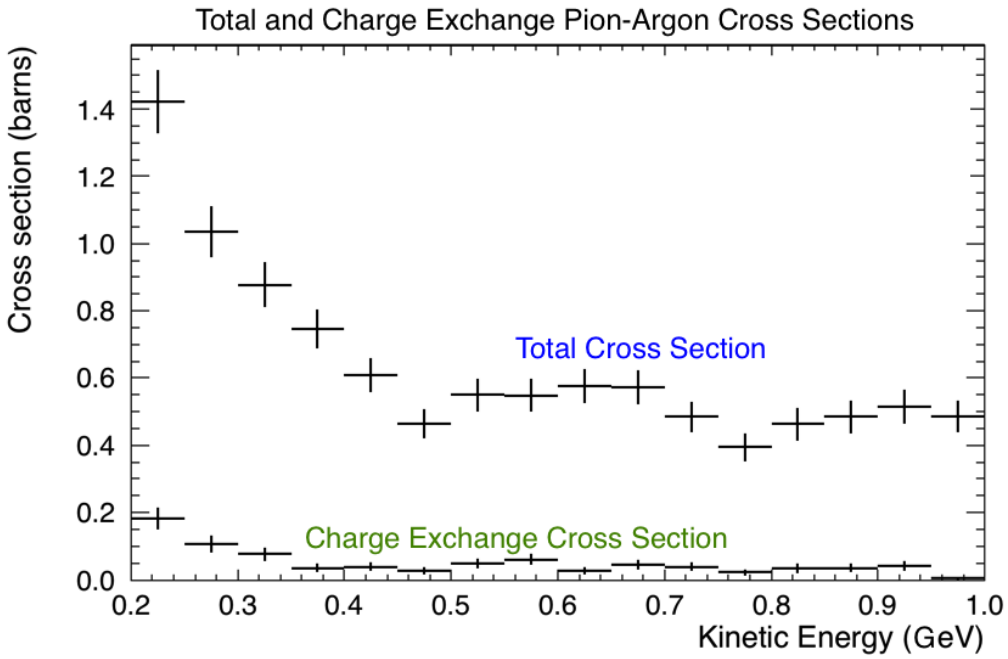

Figure 9: Monte Carlo charge exchange and total cross section measurements

12a plots this $\Delta\chi^2$, and figure 12b plots the efficiency and purity for proton acceptance by varying the cut value on $\Delta\chi^2$.

4 Results

4.1 Monte Carlo Cross Sections

Using the thin slab technique described in section 3.1.2, Monte Carlo measurements were produced for the $\pi^{\pm}$-Argon total cross section and charge exchange cross section. These measurements can be seen in figure 9. Figure 9 also illustrates the need for a high purity sample of Charge exchange events: with the background being any event that is not charge exchange, the charge exchange signal could be easily drowned out in noise if only a few background events are admitted per bin.

4.2 Vertex Finding

The vertex finding algorithm produced acceptable agreement with the simulated vertex position, as shown in figure 10. Typical detector smearing from the geometry of the wire planes is on the

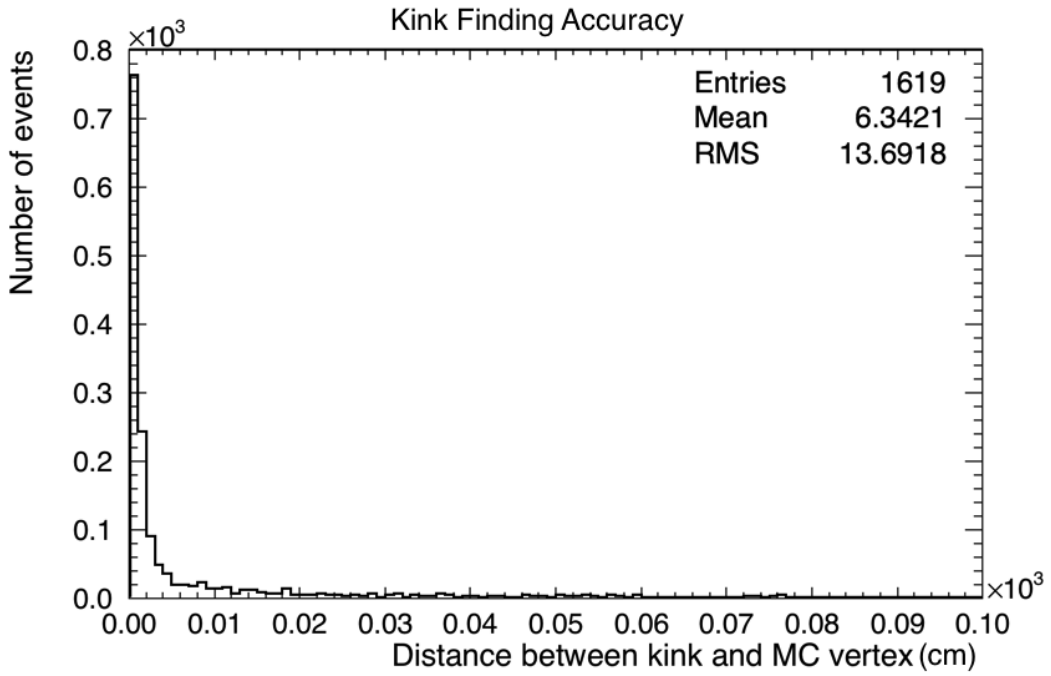

Figure 10: Agreement between MC and reconstructed interaction location for all $\pi^{\pm}$ interaction channels

order of 0-3 cm. Nearly 90% of the signal events meeting this cut, although the mean is brought up by outlier events. When reconstruction fails it does have a tendency to fail catastrophically, with greater than 10 cm of displacement between the actual and reconstructed vertex location. The 10% of events that do not meet this cut are currently unexplained.

4.3 π^0 Identification

With a reconstructed vertex established, events are classified as having a π^0 produced at that vertex or not. Figure 11 shows the efficiency and purity for various cuts to describe π^0 production. As the cuts become stricter in describing π^0 decay, efficiency is sacrificed for purity.

4.4 $\pi^{\pm}$-proton discrimination

Finally, an event with π^0 production can be rejected as charge exchange if a charged pion exits the interaction vertex. Figure 12 assesses the effectiveness of the dE/dx vs. residual range method of particle identification. In figure 12a the cut value is the confidence in the proton hypothesis, with

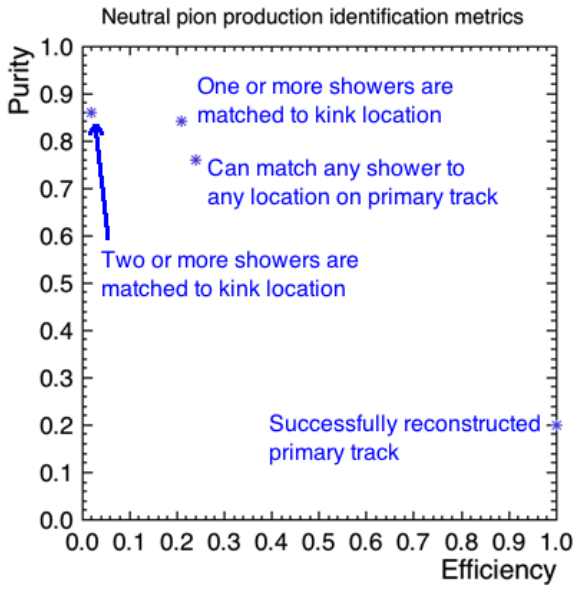

Figure 11: Efficiency and purity for π^0 identification. Annotated with cuts applied.

zero meaning that the algorithm cannot tell the difference between the likelihood of the proton or pion hypothesis, negative values being particles classified as more likely to be pions, and positive $\Delta\chi^2$ being more likely a proton. The efficiency and purity plot in figure 12b is the set of points created by iterating a cut value on $\Delta\chi^2$ from zero to 100. Because signal events allow for protons but not $\pi^{\pm}$, efficiency is the proton acceptance efficiency, and purity is the accepted particle proton purity. The high volume of pions will require a more sophisticated technique, as discussed in section 5.

4.5 Charge Exchange Classification

Finally, with efficiency and purity curves for π^0 production and $\pi^{\pm}$-proton discrimination, I can assess the accepted sample of charge exchange events using my algorithm. Charge exchange events are accepted with 8.5% efficiency and 61% purity. Before a measurement of the charge exchange cross section is made using data, the purity of this sample must be increased.

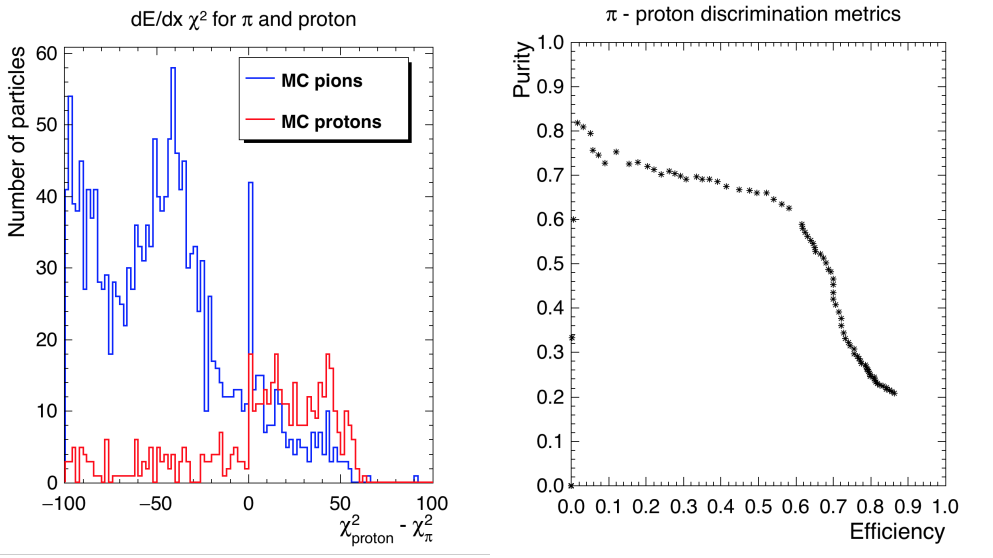

(a) $\Delta\chi^2$ test for pions and protons

(b) Efficiency and purity for cuts on $\Delta\chi^2$

Figure 12: The effectiveness of the dE/dx vs. residual range method of discriminating between pions and protons.

5 Conclusions and Future Work

The ultimate goal of this research project is to produce a measurement of the charge exchange cross section using data from LArIAT's Run II. This is a progress report on that endeavor. From a sample of Monte Carlo events with 2% charge exchange purity, a sample was selected using the algorithm outlined in this paper that increased purity to 61%. This is a success, but not the end of purity improvements. π^0 identification purity and efficiency will likely be improved by tuning the photon finding algorithm for the specific purpose of this analysis. $\pi^{\pm}$-proton discrimination will be improved by implementing an algorithm that includes momentum considerations in dE/dx particle identification, similar to Walton's work with particle identification in MINERνA [5]. One purity and efficiency are improved on both fronts of charge exchange classification, the first data measurement of the $\pi^{\pm}$-Argon charge exchange cross section will be within our reach.

References

[1] F. P. An et al., *Observation of electron-antineutrino disappearance at daya bay*, (2012).

[2] F. Cavanna et al., *Lariat: Liquid argon in a testbeam*, (2014).

[3] J. Ellis, *Tikz-feynman: Feynman diagrams with tikz*, (2016).

[4] K. A. Olive et al., *Review of Particle Physics*, Chin. Phys., C38 (2014), p. 090001.

[5] T. Walton, *A measurement of the muon neutrino charged current quasielastic-like cross section on a hydrocarbon target and final state interaction effects*, (2014).